Molecular Crystals and Liquid Crystals

Publication details, including instructions for authors and subscription information:
http://www.tandfonline.com/loi/gmcl20

Conjugated Polymers Oriented Organic Thin Films for Nonlinear Optics

Ileana Rau [a], Pawel Armatys [a], Pierre-Alain Chollet [a], Francois Kajzar [a] & Roberto Zamboni [b]

[a] CEA SACLAY, DRT/LITEN/DSEN/GENEC/L2C, Gif sur Yvette, Gifsur Yvette, France

[b] Consiglio Nazionale delle Ricerche, Istituto per lo Studio dei Materiali, Nanostrutturati-Sezione di Bologna, Bologna, Italy

Version of record first published: 16 Aug 2006

To cite this article: Ileana Rau, Pawel Armatys, Pierre-Alain Chollet, Francois Kajzar & Roberto Zamboni (2006): Conjugated Polymers Oriented Organic Thin Films for Nonlinear Optics, Molecular Crystals and Liquid Crystals, 446:1, 23-45

To link to this article: http://dx.doi.org/10.1080/15421400500383048

Mol. Cryst. Liq. Cryst., Vol. 446, pp. 23–45, 2006

ISSN: 1542-1406 print/1563-5287 online
DOI: 10.1080/15421400500383048

Taylor & Francis
Taylor & Francis Group

Conjugated Polymers Oriented Organic Thin Films for Nonlinear Optics

Ileana Rau
Pawel Armatys
Pierre-Alain Chollet
Francois Kajzar
CEA SACLAY, DRT/LITEN/DSEN/GENEC/L2C, Gif sur Yvette, France

Roberto Zamboni
Consiglio Nazionale delle Ricerche, Istituto per lo Studio dei Materiali, Nanostrutturati-Sezione di Bologna, Bologna, Italy

Preparation of oriented thin films of a series of soluble conjugated polymers and characterization of linear and nonlinear optical properties is described and discussed. The orientation of polymer chains leads to an enhanced cubic susceptibility, important for the targeted practical applications of these materials. The refractive indices and the optical birefringence of thin films were determined using the m-lines technique. The nonlinear optical properties were measured by optical third harmonic generation technique and by picosecond z-scan method. The figures of merit for the application of PPV-MDMO polymer in all optical switching are derived. The kinetics of chemical degradation of a conjugated π electron polymer was also studied and the degradation rate was measured.

Keywords: conjugated polymers; cubic susceptibility; oriented thin films; refractive indices; third harmonic generation; z-scan

INTRODUCTION

The rapid development of telecommunications calls the role for broad band and fast transmission systems. The heart of the photonic

This work was supported by the IST initiative of the European Union through the contract IST-2001-38919 – Phoenix. I. Rau would like also to acknowledge the post-doc fellowship attributed by International Relations Direction of CEA (DRI) through the EGIDE organization.

Ileana Rau on leave from POLITEHNICA University of Bucharest, Romania. Pawel Armatys on leave from Academy of Mining and Metallurgy, Krakow, Poland.

Address correspondence to Ileana Rau, CEA SACLAY, DRT/LITEN/DSEN/GENEC/L2C, Bât 451, 91191 Gif sur Yvette Cedex, France. E-mail: ileana_brandusa@yahoo.com

networks are optical switching elements which allows to manipulate the signal (routing, modulation) transmission. At the present time one uses either the direct light source modulation (laser diodes) or electronic interfaces in order to transform an electric current (or electric field) modulation into the optical wave intensity modulation by using the linear electro-optic effect. Such systems are frequency limited due to the bandwidth of electronic systems. Significantly larger transmission band can be obtained by using purely optical switching elements (intensity dependent refractive index, namely Kerr effect) and taking advantage of the fast third-order nonlinear optical susceptibility, which is enhanced in organic π electron conjugated 1D systems. Therefore a lot of effort was done, namely theoretical modeling (quantum calculations), material synthesis and processing as well as optical characterizations. More specifically, since the applications are targetted in waveguiding configuration, materials processable into good optical quality thin films with large third-order NLO properties were specially addressed [1–4]. Optimising the macroscopic Kerr susceptibility is achieved in two steps: optimising the microscopic susceptibility at the molecular level, and then optimising the packing of molecules (or polymers) in order to exploit the enhancement of cubic susceptibility in 1D conjugated systems by orienting them in the same direction. Another very important point to address is performance degradation with time, which is due to chemical – and photodegradation, namely the often observed decrease of the conjugation length induced by photoassisted oxidation.

In this paper we report results of a systematic study of linear and nonlinear optical properties of several conjugated 1D π electron systems in view of their application in all optical systems. The studied compounds were processed into thin films by solution cast technique by spinning and drawing (soluble polymers), or in the case of smaller molecules (C_{70}, AlQ_3, sexithiophene) by vacuum evaporation. The molecular order was checked by linear optical dichroism and by measuring the optical birefringence of the films. The nonlinear optical properties were studied by the optical third harmonic generation and by z-scan techniques in thin films.

PHYSICAL BACKGROUND AND QUANTIFICATION OF DEVICE PERFORMANCES

Macroscopic and Microscopic Hyperpolarisabilities

The optical switches, mentioned in Introduction, are based on change of refractive index of a given material with light intensity I_ω

at frequency ω:

$$n(\omega) = n_0 + n_2 I_\omega \tag{1}$$

where n_2 is the nonlinear index of refraction. This dependence follows from the nonlinear dependence of the macroscopic polarisation P, written in the laboratory reference frame (I, J, K), on the forcing electric field strength E. For centrosymmetric systems, we are dealing with, and in the frame of dipolar approximation it leads to (hereafter we limit us to degenerate processes only):

$$\begin{aligned} P_I(\omega) &= \chi^{(1)}_{IJ}(-\omega;\omega)E^\omega_J + \chi^{(3)}_{IJKL}(-\omega;\omega,-\omega,\omega)E^\omega_J E^\omega_K E^\omega_L + \cdots \\ &= \chi'^{(1)}_{IJ}(-\omega;\omega)E_J \end{aligned} \tag{2}$$

where $\chi^{(1)}_{IJ}$ is IJ component of the linear susceptibility and $\chi^{(n)}_{IJKL}$ is the IJKL component of the fourth rank tensor describing degenerate third-order nonlinear optical effects. The electric field (optical, DC or AC) dependent susceptibility $\chi'^{(1)}_{IJ}$ is given by

$$\chi'^{(1)}_{IJ}(E,\omega) = \chi^{(1)}_{IJ} + \chi^{(3)}_{IJKL}(-\omega;\omega,-\omega,\omega)E^\omega_K E^\omega_L + \cdots \tag{3}$$

This leads to the intensity dependence of refractive index:

$$n_{IJ}(\omega) = \sqrt{1 + \frac{\chi'^{(1)}_{IJ}}{\varepsilon_0}} \tag{4}$$

For isotropic systems and limiting the development (3) to two photon absorption (TPA) only one gets

$$n_2(\omega) = \frac{3\chi^{(3)}(-\omega;\omega,-\omega,\omega)}{4\varepsilon_0 \mathrm{c} \mathrm{n}_0^2} \tag{5}$$

where c is the speed of light and n_0 is defined in Eq. (1). In Eqs. (2) and (3) the Einstein's notation for summation is used.

Similarly, at the molecular (microscopic scale), the oscillating dipole $p(\omega)$ of molecule at frequency ω depends on the applied electric field E too. For a centrosymmetric molecule and within dipolar approximation this may be written in the molecular frame (i, j, k) as follows:

$$p_i(\omega) = \alpha_{\mathrm{ij}}(-\omega;\omega)\mathsf{E}^{\omega_\sigma}_{\mathrm{j}} + \gamma_{\mathrm{ijkl}}(-\omega;\omega,-\omega,\omega)\mathsf{E}^{\omega}_{\mathrm{j}}\mathsf{E}^{\omega}_{\mathrm{k}}\mathsf{E}^{\omega}_{\mathrm{l}} \tag{6}$$

where E_i^{ω} is the microscopic local field experienced by molecule. In media with small optical anisotropy the local field E_i^{ω} is related to the macroscopic one by the Lorentz equation:

$$E_i^{\omega} = f^{\omega} E_j^{\omega} \tag{7}$$

with

$$f^{\omega} = \frac{n_{\omega}^2 + 2}{3} \tag{8}$$

being the local field factor.

For practical applications important is the value of the nonlinear index of refraction n_2 or, in other words, the value of cubic susceptibility $\chi^{(3)}$ (cf. Eq. (5)). For a single crystal and for noninteracting molecules the linear and NLO susceptibilities can be obtained by transforming the molecular hyperpolarizabilities from the molecular reference frame to the laboratory system. For the cubic susceptibility one gets in this way the following formula:

$$\chi^{(3)}_{IJKL}(-\omega;\omega,-\omega,\omega) = N(f^{\omega})^4 a_{iI} a_{jJ} a_{kK} a_{lL} \gamma_{ijkl}(-\omega;\omega,-\omega,\omega) \tag{9}$$

In this equation, N is the volumic concentration of molecules (or polymer repeat units), $a_{iI} = \cos(i,I)$ are the projection factors (Wigner's rotation matrix elements) arising from the change of frame (i, j, k) $\rightarrow$ (I, J, K). Just the macroscopic NLO susceptibility depends not only on the molecular second hyperpolarizability value g, optimized by the molecular engineering, but also on the way how the molecules arrange between them to form a given material. This is optimized by the material engineering approach.

For partly ordered systems, we are dealing with, Eq. (9) is not valid. In that case the cubic suceptibility is given by the orientational average of molecular hyperpolarizability tensor components:

$$\langle \chi^{(3)}(-\omega;\omega,-\omega,\omega)\rangle_{IJKL} = N\langle (f^{\omega})^4 \gamma_{ijkl}(-\omega;\omega,-\omega,\omega)\rangle_{IJKL} \tag{10}$$

Equation (10) is very complex and its use requires the knowledge of all components of second hyperpolarizability γ as well as the orientation distribution function of molecules. It becomes much simpler in the case of conjugated in 1D polymers or molecules. In that case the γ_{xxxx} tensor components in the π electron conjugation direction x is enhanced and the others can be neglected with respect to this one.

In that case Eq. (10) reduces to a much simpler one:

$$\langle \chi^{(3)}(-\omega;\omega,-\omega,\omega)\rangle_{IJKL} = N(f^{\omega})^4 \gamma_{xxxx} \langle \cos^4 \Theta \rangle_{IJKL} \tag{11}$$

where Θ is the angle between the molecular axis (conjugation direction) and a chosen direction in the laboratory reference frame.

Thus the strategy for optimising the performances of devices, directly connected to the magnitude of $\chi^{(3)}$ susceptibility consists on:

a) *increasing the value of the molecular second hyperpolarizability* $\gamma(-\omega;\omega,-\omega,\omega)$ *through molecular engineering*, as already mentioned. In conjugated π electron systems γ depends strongly on the conjugation length (L_c) and the dependence is given by the scaling law [5]

$$\gamma_{xxxx} \propto L_c^{\alpha} \tag{12}$$

where $\alpha = 5 \div 7$ according to the theoretical calculations.

The scaling law (Eq. (12)) was tested experimentally and theoretically by studying the dependence of the hyperpolarizability γ on number of π electrons [6] or the number of conjugated bonds N [7]

$$\gamma_{xxxx} \propto \mathrm{N}^{\alpha_N} \tag{13}$$

Note that the conjugation length L_c does not extend on the whole spatial extension of the oligomer or polymer (number of conjugated bonds), with the consequence that $\alpha_{\mathrm{N}} < \alpha$. Depending on polymer it saturates for some number of conjugated bonds [7].

It was found that for the conjugated in one dimension π electron polymers [8]:

$$\alpha_N = 3 \div 6.3 \; - \text{ theory}, \qquad \text{and}$$
$$\alpha_N = 2.3 \div 4.5 \; - \text{ experiment}$$

b) *increasing the volumic concentration N of active chromophores or monomer units.* This is achieved by material processing and the increase is limited by the size of molecules, side groups, etc. In the case of solid solutions of active NLO molecules their concentration is limited by their aggregation, which leads to the unwanted increase of propagation losses. In that case an increase of the chromophore concentration may be obtained by covalently attaching them on the polymer backbone.

c) *optimising the configurational average* $\langle cos^4 \Theta \rangle$ (cf. Eq. (11)). This can be achieved by orientation of molecules or polymer chains. Depending on the amount of order $\langle \cos^4 \Theta \rangle$ takes values between

0.2 (isotropic distribution) and 1 (monoorientation):

$$\langle \cos^4 \Theta \rangle = \begin{cases} 1 - MONOORIENTATION \\ \frac{3}{8} - 2 - D\ DISORDER \\ \frac{1}{5} - 3 - D\ DISORDER \end{cases}$$

It corresponds to the $\chi^{(3)}$ susceptibility variation by a factor of 5 between these two extreme cases and similarly for the nonlinear index of refraction n_2. Thus by simply orienting the polymer chains (or 1D conjugated molecules) one can improve significantly the device performances.

Figures of Merit

The applicability of a given material in all optical switching devices depends not only on the value of the Kerr susceptibility $\chi^{(3)}(-\omega;\omega,-\omega,\omega)$ (or in other terms the value of nonlinear index of refraction n_2) but also on beam propagation losses. Two kinds of losses are present:

i) *linear*, arising from linear absorption due to the presence of impurities, light scattering on scattering centers (e.g. aggregates, crystallites, etc), absorption by harmonics of vibronic. This one is described by the linear absorption coefficient $\alpha^{(1)}$.

ii) *nonlinear absorption*, arising from the multiphoton transitions to excited states. In the presence of such an absorption the nonlinear index of refraction is complex:

$$n_2 = n_2^r + i\kappa_2 \tag{14}$$

where n_2^r is the real part and κ_2 is the extinction coefficient. In the presence of higher order absorption than TPA both depend on the light intensity. In order to realize an all optical switching device, the material absorption (linear, TPA and/or higher order induced) has to be weaker than the phase shift induced by Kerr effect, for a given optical path length.

– For linear absorption, the first figure of merit (FOM) W has to be larger than unity

$$W = \frac{n_2^r I}{\alpha^{(1)}\lambda} \gg 1 \tag{15}$$

– For TPA (and or higher order) absorption the second figure of merit T must be smaller than unity.

$$T = \frac{4\pi\kappa_2}{n_2^r} < 1 \tag{16}$$

Thus, in order to satisfy the above requirements it is necessary to have materials with sufficiently large real part of nonlinear index of refraction n_2^r, small nonlinear (two photon or higher orders) absorption and good propagation properties (small $\alpha^{(1)}$).

The techniques used usually for fabrication of oriented thin films are:

- Langmuir – Blodgett techniques (2D order)
- Shear technique (solution growth) – used with topochemically polymerising polymers like polydiacetylene (PDA)
- Stretching (free standing films; films on stretchable substrate)
- Epitaxy (molecular epitaxy) – again working with topochemically polymerising polymers like PDA or with small molecules.

MATERIALS

Polymers and Molecules

The following, soluble, π electron conjugated polymers were used in this study, together with AlQ_3, α – sextithiophene and fullerenes C_{70} used for vacuum deposition:

- Poly(2-methoxy-5-(3′,7′-dimethyloctyloxy)1,4 phenylenevinylene) (PPV-MDMO)
- Poly(3-butyl thiophene) (PBT)
- Poly(3-octyl thiophene) (POT)
- Polyaniline (PANI)

The chemical structures of the studied polymers and molecules are shown in Figure 1. PPV-MDMO is a commercial polymer, provided by Aldrich, while the others were synthesized in the laboratory. The polymers were dissolved in appropriate solvents (1,1,2-trichlorethane, chlorobenzene or 1-methyl-2-pyrolidinone) and the solutions were filtered with Millipore filters (1 μm). The substrates were carefully cleaned using a strong detergent, ultrasounds, Millipore water and annealing in an oven (350°C).

First the thin films were deposited by spinning. Only PPV-MDMO and poly(3-alkyl thiophene) solutions adhere well to the substrate

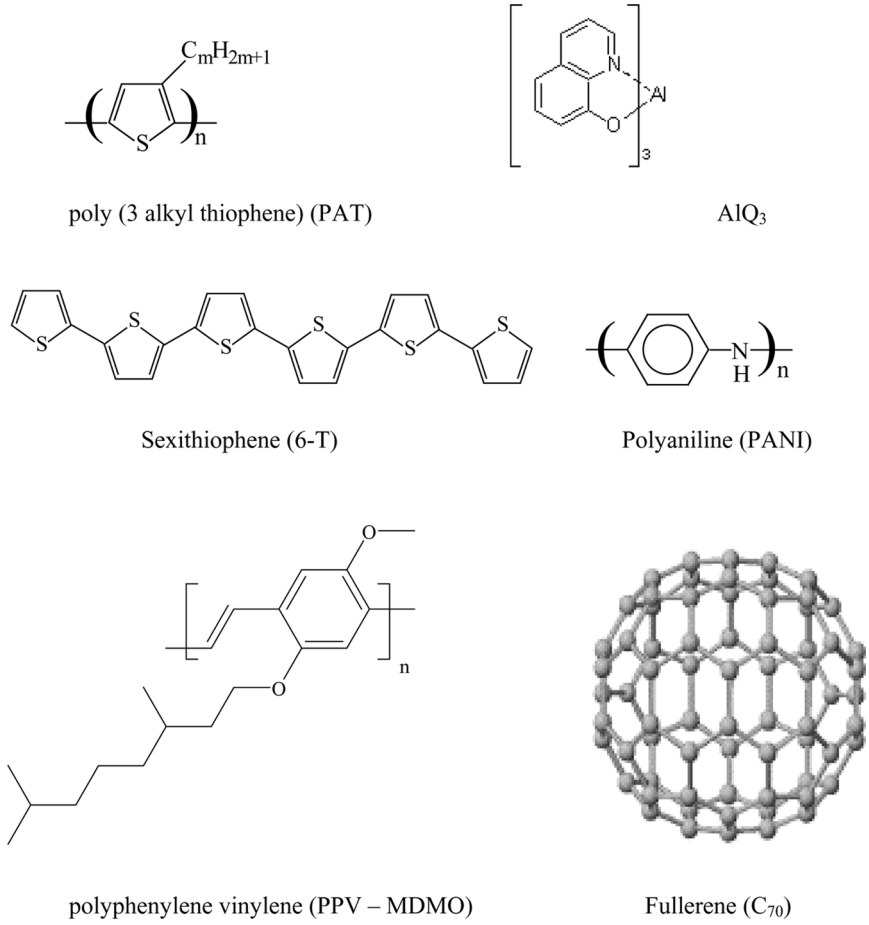

FIGURE 1 Chemical structure of studied polymers and molecules.

and form good optical quality thin films. The spinning technique is very frequently used in thin film fabrication for optical applications and usually leads to either isotropic or partly ordered 2D thin films with polymer chains oriented preferably parallel to the substrate (cf. e.g. Koynov *et al*. [9]).

In order to obtain a 1 D orientation of polymer chains we decided to take advantage of the hydrodynamic force when drawing a substrate from polymer solution. This force could order the chains parallel to the drawing direction. We have set up a drawing system allowing a precise control of its speed. This technique is detailed in a former paper [10].

Spectral Characterisation – Kinetic Study

An important problem encountered with conjugated molecules and polymers is their chemical stability. The presence of oxygen can induce chemical reactions leading to the decrease of conjugation length and consequently decrease of nonlinear index of refraction, modifying linear optical properties too. Also intense laser pulses may not only favorize these chemical reactions through opening of conjugated bonds via multiphoton absorption processes but also destroy molecules due to the dielectric breakdown.

We have performed experiments which show that even changing the film deposition technique (spin-coating → drawing) affects the stability. This was addressed for the poly-phenyl-vinylene derivative (PPV-MDMO) thin films made by spinning and by drawing. The absorption spectra, recorded in time, for spun films show a constant decrease of the optical density with a systematic shift of the absorption maximum wavelength towards shorter wavelengths. The decrease of optical absorption is due to the chemical degradation of polymer (decrease of the number of active species) and the shift is a fingerprint of the shortening of the conjugation length (cf. Fig. 2) most likely resulting from the backbone oxidation.

One can assume reasonably that this degradation can be described by the first order kinetics law:

$$\frac{dc}{dt} = -kc \tag{17}$$

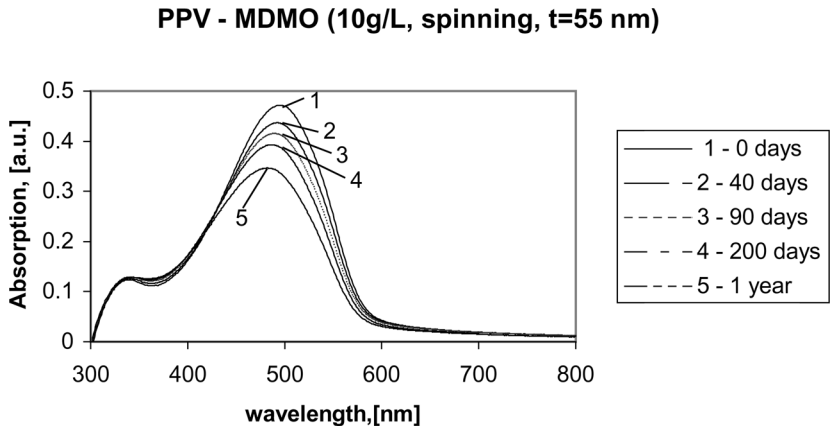

FIGURE 2 Temporal variation of optical absorption spectra of a PPV-MDMO spun film. The absorption below 350 nm is falsified by not well balanced contributions from thin film substrate and from the glass reference.

where c is the concentration of active species, t is time and k is the degradation rate constant. Knowing that the optical density A is a function of c (Lambert–Beer law), after integration, Eq. (17) becomes

$$\ln A = -k\,t + \text{const} \tag{18}$$

where A is the measured absorbance at time t. Figure 3 shows a least square fit of Eq. (18) to experimental data for a thin film of MDMO-PPV made by spinning method. A good agreement is observed, showing that indeed the thin film degradation takes place according to the first order kinetics law. It follows from it that for this polymer the degradation rate constant $k = 9 \times 10^{-4}$ days^{-1} and the half time period $t_{1/2} = 770$ days.

In the case of thin films of PPV-MDMO drawn from the polymer solution the chemical degradation takes place in two steps (cf. Figs. 4, 5). In the first period of time (up to about 120 days) the optical density of these films decreases and can be more or less described by the first order kinetic law, as in the case of spun films. Then it starts to increase showing that most likely a reorientation of polymer chains takes place, as it will be discussed later.

Evidently the chemical degradation process in thin film depends on the thin film morphology, as expected, this one depending on the preparation method.

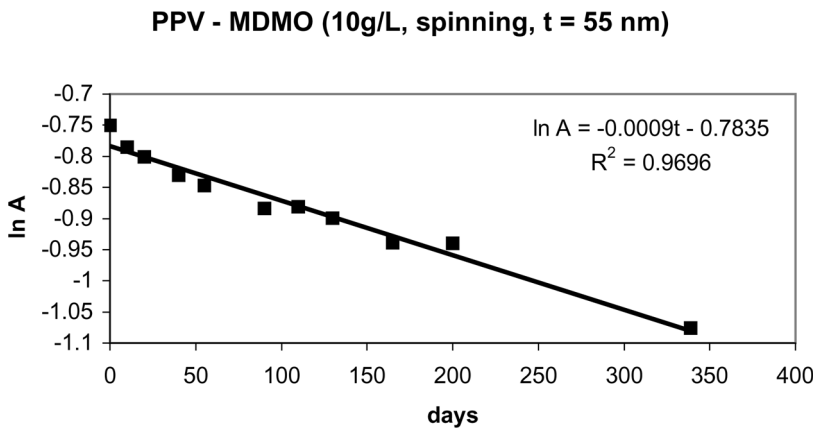

FIGURE 3 The measured (squares) and fitted with first order kinetics law (solid line) variation of optical density (in logarithmic scale) for a spun film of PPV-MDMO.

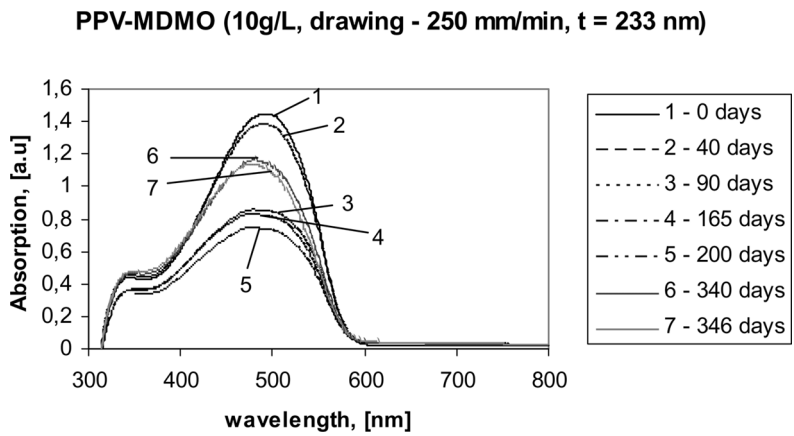

FIGURE 4 Temporal variation of optical absorption spectra of a solution drawn thin film of PPV – MDMO. Other details as in Figure 2.

Solution Drawn Thin Films

As it was discussed and shown in a preceding paper [10] the solution drawn films are partly ordered with polymer chains preferably oriented in the drawing direction. The amount of orientation was described by the order parameter B defined as [10]:

$$B = \frac{A_{\parallel} - A_{\perp}}{A_{\parallel} + A_{\perp}} \tag{19}$$

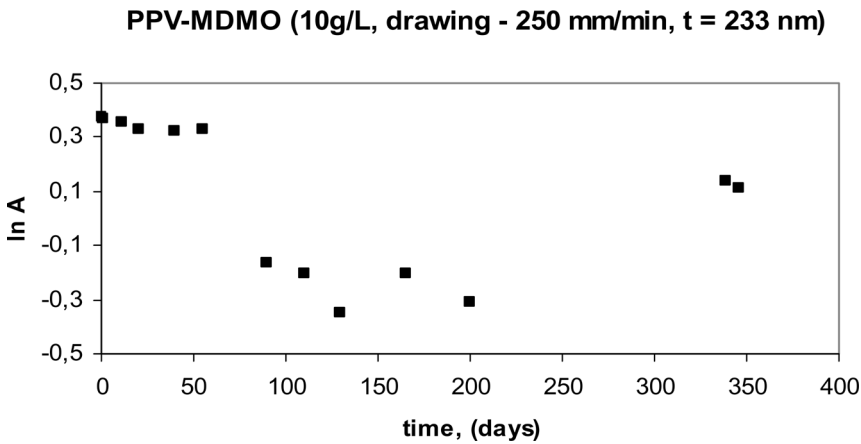

FIGURE 5 The measured (in logarithmic scale) variation of optical density for a solution drawn thin film of PPV-MDMO.

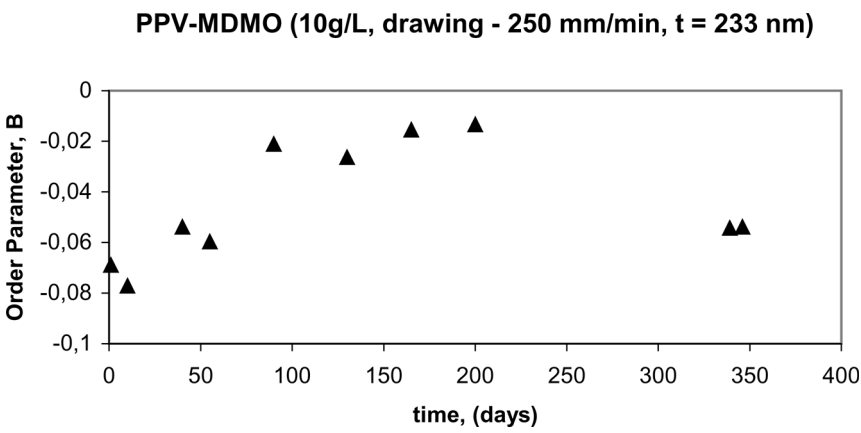

FIGURE 6 Temporal variation of the order parameter B for a solution drawn thin film of PPV-MDMO.

were $A_{\perp}$ and $A_{\parallel}$ are optical densities perpendicular and parallel to the drawing direction, respectively. The B parameters between -0.24 (thin films of PPV-MDMO) and $+0.07$ (thin films of poly(3-octyl thiophene) were observed. The negative value of B means that chains orient perpendicular to the drawing direction. With time the molecules tend to disorganize them, but apparently, after certain time, they start again to organize them (Fig. 6). This behaviour could be explained by the fact that during the drawing process the polymer chains were forced to align. Due to the degradation and most likely the shortening of polymers the constraint created during drawing are released and the polymer chains reorient. It coincides with the observed decrease of the order parameter B, as it is seen in Figure 6.

LINEAR OPTICAL PROPERTIES AND PROPAGATION LOSSES

Refractive Indices

The knowledge of refractive index of materials used in the devices is very important for different reasons. Most of these devices are optical guides having a core and cladding. The extension of the electromagnetic field outside the core (in the cladding) is directly connected with the difference between the core and cladding refractive indices. The larger is this value, the more confined in the core is the electromagnetic field. Optical coupling between two neighbour guides (and switching between them) increases with the overlap of the electromagnetic field of mode(s) propagating in these guides. Moreover, the transmission coefficient from one first guide to another following the

first is also connected with the overlap integral of the modes supported by these guides. This overlap integral is mostly governed by the transverse geometry and refractive indices of the constituents of the guide.

The refractive indices of thin films were determined by the m-lines technique. In some cases the Fabry – Perot interferences as well as the Kramers – Kroning relations were used. The last method allows to determine the refractive indices within the absorption band where the two former ones are not applicable.

The spinning technique leads usually to partially ordered in 2D thin films with polymer chains oriented preferably parallel to the substrate plane. A best way to check such an order is by measuring the optical birefringence by checking the anisotropy of the index of refraction. In order to do this we used the m-lines technique and we observed in the case of PPV-MDMO and sexithiophene an important birefringence [10] while for the films of C_{70}, AlQ_3 (both made by vacuum evaporation technique) and PBT (spinning method), no birefringence is observed, showing an isotropic distribution of molecules (C_{70}, AlQ_3) or polymer chains (PBT, cf. Figs. 7–9).

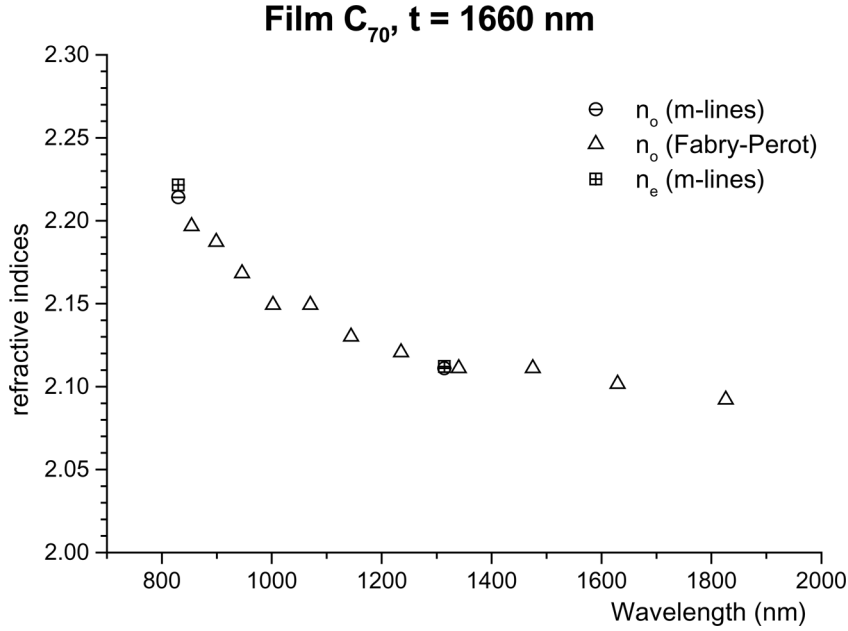

FIGURE 7 Refractive index dispersion of a vacuum evaporated thin film of C70 with thickness of 1660 nm as determined by the m-lines technique (squares) and by Fabry–Perot interferences (triangles).

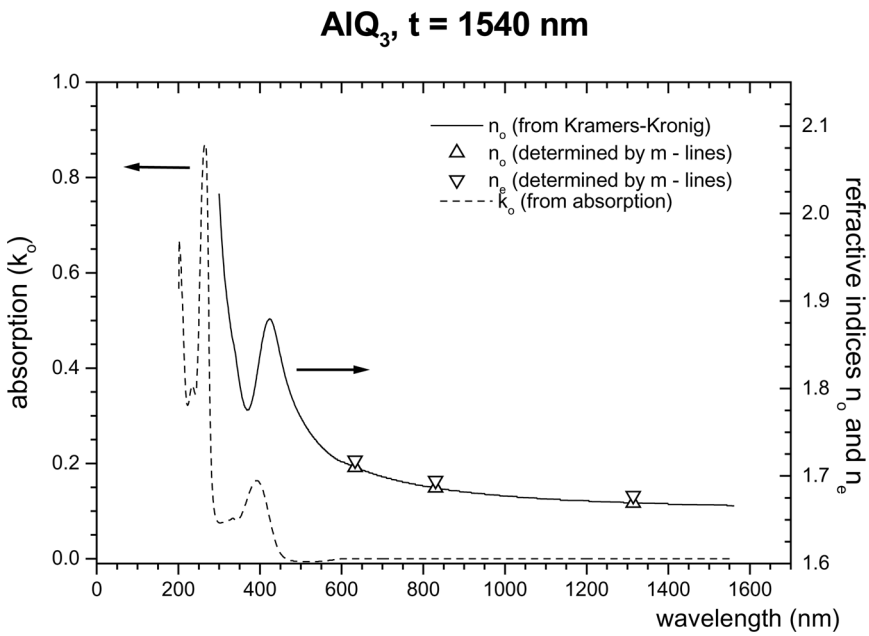

FIGURE 8 Refractive index dispersion of a vacuum evaporated thin film of AlQ_3 as determined by m-lines technique (triangles) and by Kramers–Kronig relations (solid line). The dashed line shows the extinction coefficient.

Propagation Losses

In waveguides, the optical losses can easily appear since the propagation length extends upon thousands of wavelengths. They can be independent of light intensity and due to intrinsic absorption of the active molecule. This absorption can be lowered by shortening the conjugation length, at the expense of $\gamma(-\omega;\omega,-\omega,\omega)$ magnitude.

The propagation losses were measured by imaging the scattered intensity of a propagating mode in thin film. Scattering by itself contributes to the losses. Its attenuation is thus measure of the travelling beam attenuation due to both absorption and scattering. By this method the losses of a perfect film (no absorption and no scattering) cannot be measured.

Figure 10 shows a photograph of a guided mode in a PPV-MDMO film at 830 nm as visualized by a CCD camera. The propagation losses, derived from the attenuation of scattered intensity (cf. Fig. 11) are equal to 0.6 dB/cm at this wavelength.

The linear absorption coefficient $\alpha^{(1)}$ in Eq. (15) contains not only absorption *senso stricto* but also losses arising from scattering. It is

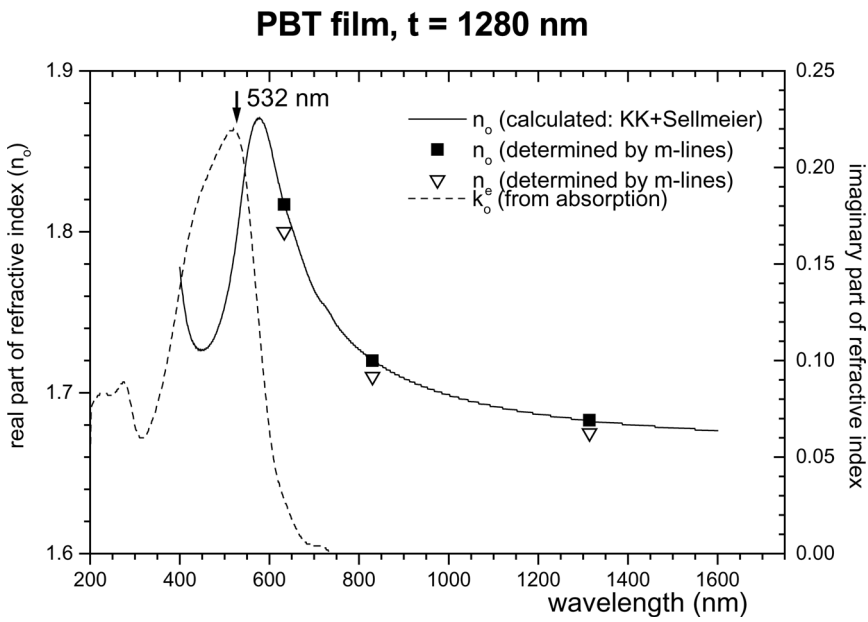

FIGURE 9 Refractive index dispersion of a vacuum evaporated thin film of PBT as determined by m-lines technique and by Kramers–Kronig relations.

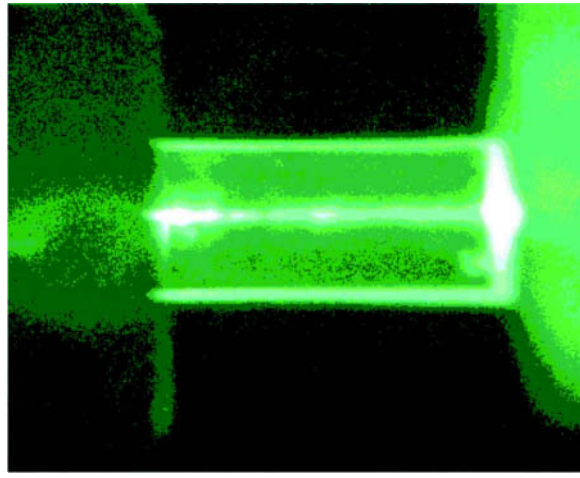

FIGURE 10 Image of guided mode with 830 nm wavelength propagating in a spun 2500 nm thin film thick of MDMO-PPV film.

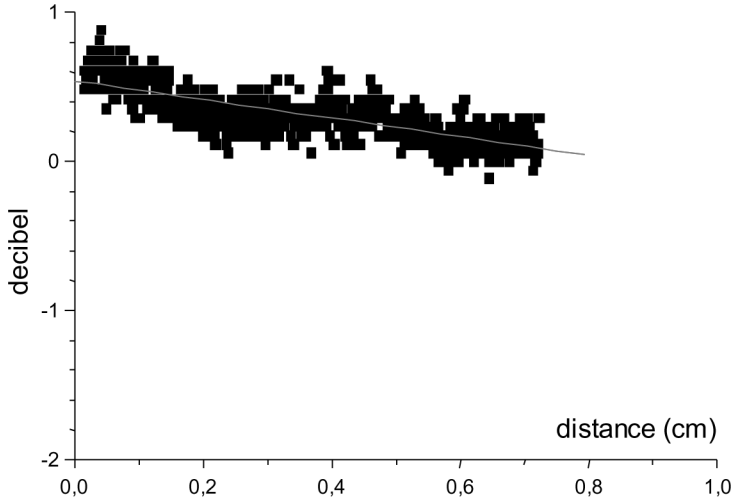

FIGURE 11 Linear fit (0.6 dB/cm) at $\lambda = 830$ nm of the experimental results obtained for a film of PPV-MDMO on silica substrate. Other details as in Figure 10.

is linked to the propagation losses PL by the following relation:

$$\alpha^{(1)} = \frac{PL}{10}\ln(10) \tag{20}$$

where PL is expressed in usually used units (dB/cm) and $\alpha^{(1)}$ in cm^{-1}. For the studied PPV-MDMO film (PL = 0.6 dB/cm) we obtain $\alpha^{(1)} = 0.14\,cm^{-1}$.

NONLINEAR OPTICAL PROPERTIES

Nonlinear Index of Refraction and Two Photon Absorption

The nonlinear index of refraction was deduced from the Z-scan measurements [11] by measuring the transmitted intensity with sample translated across the focal point of focussed laser beam (cf. Fig. 12). Due to the nonlinear refraction the sample acts as a lens which is more effective close to focus and moves the focal point of lens towards ($n_2 < 0$) or backwards ($n_2 > 0$) increasing or decreasing the convergence of the propagating beam at a given plane after the focus. It results in an oscillation of the transmitted intensity when an aperture is interposed between the sample and the detector (cf. Fig. 12). If no aperture is interposed between the sample and the detector there is no oscillation but only decrease of the transmission due to the nonlinear absorption in the sample.

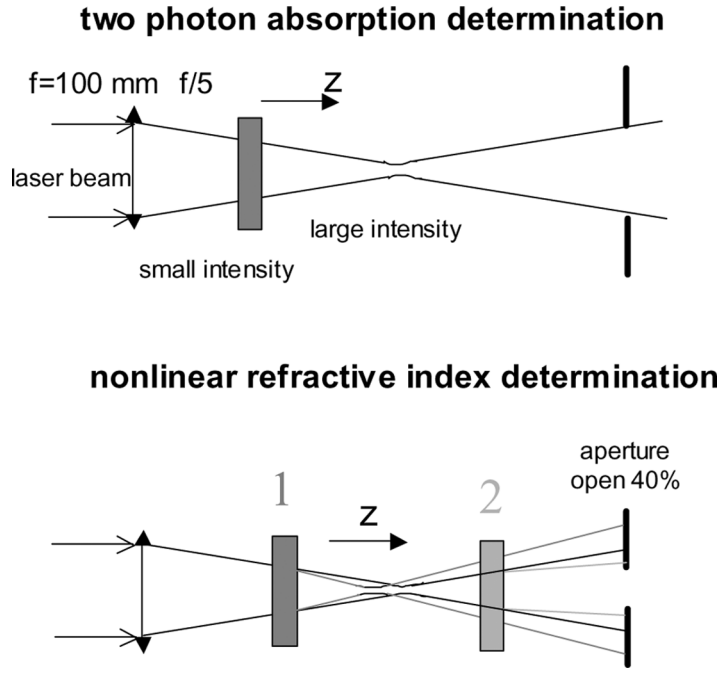

FIGURE 12 Schematic representation of the Z-scan method.

Figures 13a and 13b show the closed aperture (40% of the diaphragm transmission) and the open aperture Z-scan spectra of a PPV-MDMO film. In order to eliminate the influence of optical defects in the film the spectra are normalized to that measured at the lowest fluence. These should be intensity independent. All Z-scan measurements were done at 1064.2 nm using a pulsed mode locked Nd:YAG laser with the following characteristics: $\lambda = 1\ 064$ nm, beam waist $= 30\ \mu$m and pulse duration 30 ps. In all cases the fluence dependence was measured in order to check a possible damage to the sample at these beam energy levels. All reported results were obtained working well below the damage levels.

In order to deduce the nonlinear extinction coefficient we checked out the linearity of the variation of reciprocal transmission (open aperture) versus intensity (cf. Fig. 14). It allows to determine the two photon absorption coefficient, defined through the transmission variation through a nonlinear medium.

$$\frac{\partial I}{\partial z} = -\alpha^{(2)} I^2 \tag{21}$$

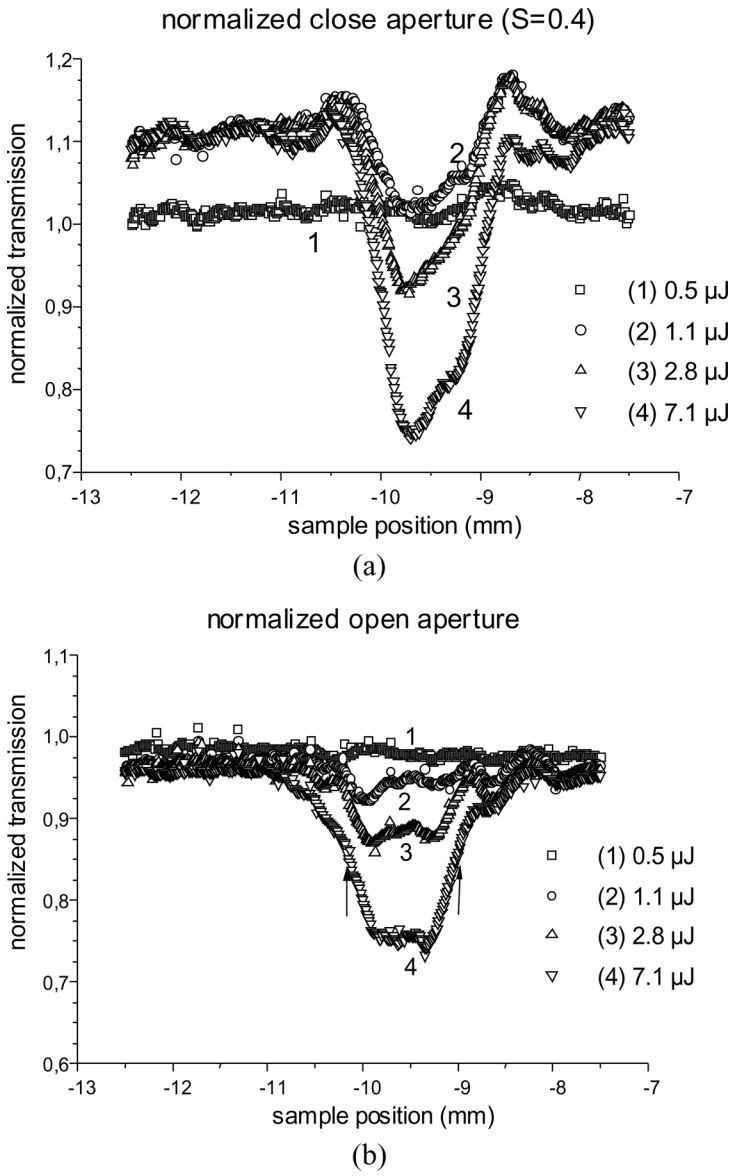

FIGURE 13 Z-scan spectra of a spun 3000 nm thick PPV-MDMO film.

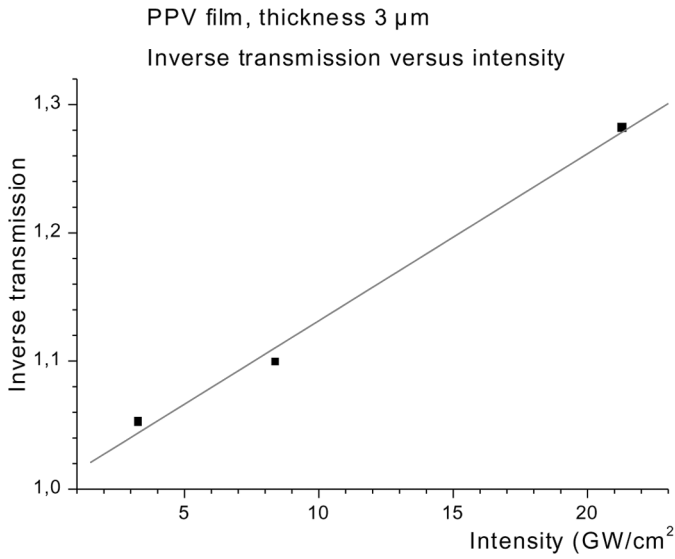

FIGURE 14 Intensity dependence of inverse of transmission for spun, 3 µm thick, film of PPV-MDMO.

where $\alpha^{(2)}$ is the two photon absorption coefficient, linked to the two photon nonlinear extinction coefficient (cf. Eq. (14)) through the following relation:

$$\alpha^{(2)} = \frac{4\pi\kappa_2}{\lambda} \tag{22}$$

For higher than two absorption processes the TPA coefficient $\alpha^{(2)}$ depends on intensity. It follows from Eq. (21) that for a sample with thickness l the inverse of transmission is given by:

$$\frac{1}{T(t)} = 1 + \alpha^{(2)} l I(0) \tag{23}$$

By fitting this dependence (cf. Fig. 14) one can determine the $\alpha^{(2)}$ coefficient for a given sample and presently $\alpha^{(2)} = 40\,\mathrm{cm/GW}$ for the studied PPV-MDMO thin films. With relation (22) it gives at $\lambda = 1064.2\,\mathrm{nm}$ the corresponding $\kappa_2 = 3 \times 10^{-13}\,\mathrm{cm^2/W}$.

Comparing the Z-spectra of PPV-MDMO film (Fig. 15) with those of toluene – used as standard (cf. Fig. 16) we expected to have the extrema of transmission at the position of arrows. The Z-scan spectrum begins by a positive peak, which is in favour of a negative value for n_2.

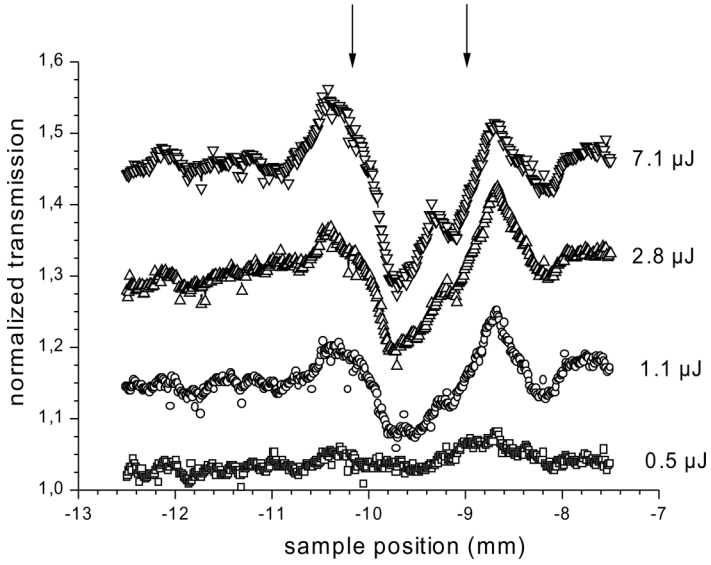

FIGURE 15 Z-scan spectra of a 3 mm thick film of PPV-MDMO at different fluences.

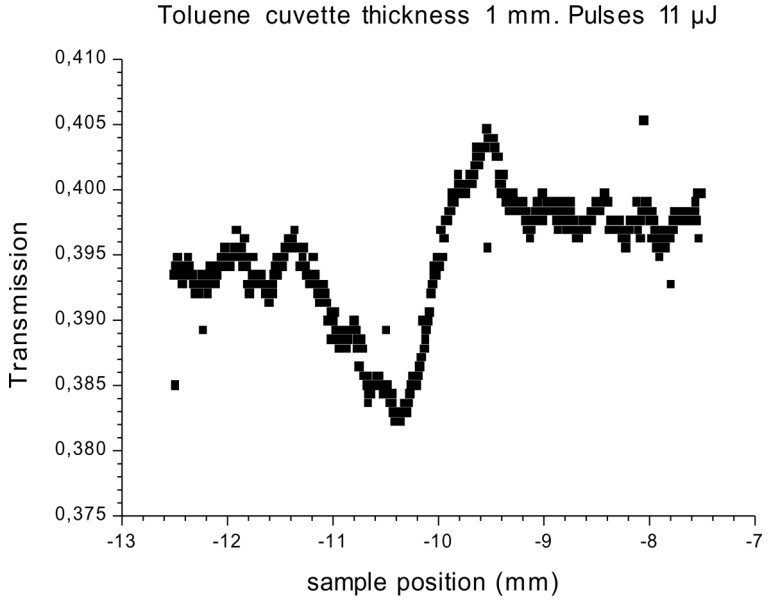

FIGURE 16 Z-scan spectrum for toluene used for calibration ($n_2 = 0.82 \times 10^{-14}\,cm^2/W$).

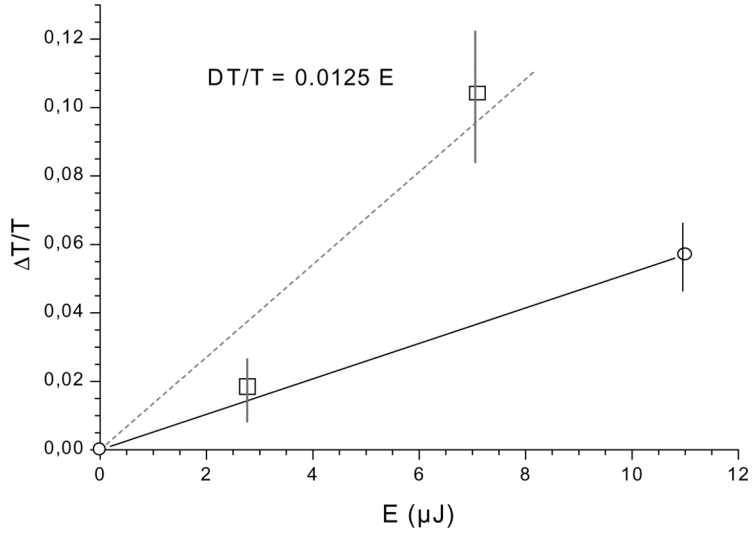

FIGURE 17 Fluence dependence of the Z-scan signals from a 3 μm thick PPV-MDMO film (squares and dashed line) and from a 1 mm thick cell filled with toluene (open circle and solid line).

By comparison of the Z-scan signals of PPV-MDMO (cf. Fig. 17) with those of toluene one obtains n_2 of the order of $10^{-12}\,cm^2/W$. This value is about two orders of magnitude larger than the used standard value for calibration ($n_2(\text{toluene}) = 0.82 \times 10^{-14} cm^2/W$) [12].

Third Harmonic Generation Measurements

It is well known that the Z-scan technique doesn't allow to discriminate between different contributions to nonlinear refraction such as of practical interest fast electronic and much more slower thermal dilatation effects. In order to determine the electronic part of cubic susceptibility we used the optical third harmonic generation technique. The details are reported in the former paper [10]. Table 1 summarizes the results obtained for thin films of different studied compounds. The nonlinear index of refraction is derived from Eq. (4) using for Kerr susceptibility $\chi^{(3)}(-\omega;\omega,-\omega,\omega)$ the value obtained from THG measurements at the same wavelength ($\chi^{(3)}(-3\omega;\omega,\omega,\omega)$). This is an approximation, which in part is justified by the fact that the two photon resonances contribute in similar way to both susceptibilities at the given wavelength [13]. We note that all studied conjugated polymer films, together with vacuum evaporated films of sexithiophene and C70, exhibit, within the above mentioned approximation, a

TABLE 1 Cubic Susceptibility $\chi^{(3)}(-3\omega;\omega,\omega,\omega)$ for Spun Films of Selected Studied Polymers and Macromolecules Together with Thicknesses and Refractive Indices at Fundamental and Harmonic Wavelengths as well as the Nonlinear Index of Refraction Derived from THG Data

Polymer	Concentration preparation	Thickness (nm)	n_ω	$n_{3\omega}$	$\chi^{(3)}$ $(-3\omega;\omega,\omega,\omega)$ 10^{-19} (m/V)	$n_2(\omega)$ interfered from $\chi^{(3)}$ 10^{-12} (cm^2/W)
PPV-MDMO	25 g/L spinning	273	1.635	1.419	3.2 ± 0.3	0.25 ± 0.02
PBT	50 g/L spinning	333	1.694	1.436	4.4 ± 0.4	0.34 ± 0.03
AlQ_3	evaporation	1550	1.675	1.793	0.31 ± 0.03	0.024 ± 0.003
C_{70}	evaporation	1660	2.149	1.816	4.2 ± 0.4	0.32 ± 0.03
Sexi-Thiophene	evaporation	160	1.969	1.506	3.2 ± 0.3	0.25 ± 0.03

comparable nonlinear index of refraction $n_2 \approx 3 \times 10^{-13} cm^2/W$. This value is about one order of magnitude smaller for AlQ_3 thin film. For PPV-MDMO thin films, for which Z-scan determinations were also done, the Z-scan value is about three times larger than that derived from THG measurements.

CONCLUSIONS

In conclusion of the present study we may say that:

- The kinetic study for the MDMO-PPV films shows that their degradation rate depends on film morphology, as expected. On the other hand the film morphology depends on its preparation technique.
  - the spun films degradation follows the first order kinetic law
  - two steps degradation process, with an alteration of the degree of order, takes place in the case of solution drawn thin films.
- Various conjugated materials (PPV-MDMO, PBT, α-6T) present comparable optical nonlinearities, contrary to AlQ_3, whose conjugation extension is significantly smaller.
- Films of good optical quality can be made by spin coating of PPV-MDMO. These films exhibit also a 2D order in the substrate which matches with TE polarization, a property interesting for device applications.
- Z-scan technique and third harmonic generation (THG) are complementary for measuring optical nonlinearities since the former is sensitive to all kind of contributions to n_2, while THG is only sensitive to electronic contributions. In the present case a rough estimates gives n_2(Z-scan) $\sim 3n_2$(THG) in the case of PPV-MDMO films. It's a fairly good agreement.

- We have calculated the figures of merit parameters T and W for PPV-MDMO thin films. Using the parameters determined in this study ($n_2^r = 10^{-12}\,cm^2/W$, $\kappa_2 = 3 \times 10^{-13}\,cm^2/W$, $\alpha^{(1)} = 0.14\,cm^{-1}$) one obtains $T = 3.8$ and $W > 600$ for beam intensity $I > 1\,GW/cm^2$. The relatively large value of T parameter is due to a large two photon absorption coefficient, which in thin films may be overestimated. Indeed, in solution and at the same wavelength we have found the β coefficient, extrapolated to bulk value, about four times smaller than in thin films. It gives the T coefficient ca. 1 showing that PPV-MDMO is potentially a good candidate for all optical switching applications at 1064 nm, provided that a necessary effort is done in thin film fabrication. It agrees with the measurement and conclusions obtained by Koynov and coworkers [14] from nonlinear m-lines study on another PPV derivative.

REFERENCES

[1] Kuzyk, M. & Dirk, C. (Eds.) (1998). *Characterization Techniques and Tabulations for Organic Nonlinear Optical Materials*, Marcel Dekker, Inc.: New York.

[2] Richardson, T. (Ed.) (2000). *Functional Polymers and Polymeric Materials*, John Wiley & Sons: Chichester.

[3] Graja, A., Bulka, B., & Kajzar, F. (2002). *Molecular Low Dimensional- and Nano-Structured Materials for advanced applications*, NATO Science Series 2, Kluwer Academic Publishers: Dordrecht.

[4] Kajzar, F. & Rau, I. (2004). Organic nonlinear materials. In: *Encyclopedia of Modern Optics, Materials for Nonlinear Optics*, Guenther, R. D., Steel, D. G., & Bayvel, L. (Eds.), Elsevier: Oxford, 42–60.

[5] Rustagi, K. C. & Ducuing, J. (1974). *Opt. Commun.*, *10*, 258.

[6] Devonald, D. P., Ferguson, I., Hutchings, M. G., Kajzar, F., Messier, J., Malaney, K., & Sentein, C. (1997). *Nonl. Optics*, *17*, 305.

[7] Samuel, I. D. W., Ledoux, I., Dhenaut, C., Zyss, J., Fox, H. H., Schrock, R. R., & Silbey, R. J. (1994). *Science*, *265*, 1070.

[8] Kajzar, F. (1993). *Nonl. Optics*, *5*, 329.

[9] Koynov, K., Bahtiar, A., Ahn, T., Bubeck, C., & Horhold, H. H. (2004). *Appl. Phys. Lett.*, *84*, 3792.

[10] Rau, I., Chollet, P. A., Kajzar, F., & Zamboni, R. (2005). Oriented Conjugated Polymer Thin Films for all Optical Switching Applications, Proceed. SPIE, vol. 5724, 259.

[11] Van Stryland, E. W. & Sheik-Bahae, M. (1998). Z-scan. In: *Characterization Techniques and Tabulations for Organic Nonlinear Optical Materials*, Kuzyk, M. & Dirk, C. (Eds.), Marcel Dekker, Inc.: New York, 665.

[12] For calibration we used toluene, whose nonlinear index of refraction $n_2 = 0.82 \times 10^{-14}\,cm^2/W$ was determined by comparison with CS_2 and its literature value $n_2 = 3.1 \pm 0.2 \times 10^{-14}\,cm^2/W$ (Ref. 11).

[13] Orr, B. J. & Ward, J. F. (1971). *Mol. Phys.*, *20*, 513.

[14] Koynov, K., Goutev, N., Fitrilawati, F., Bahtiar, A., Best, A., & Bubeck, C. (2002). *J. Opt. Soc. Am. B*, *19*, 895.